Electronic Supplementary Material (ESI) for Green Chemistry.

Supplementary information

Scalable Lignocellulosic Xerogel by Alkali Freezing and Ambient Drying

Qiaoling Huang [a], Zerong Li [a], Jialong Hu [a], Wei Wang [a,b], and Wei Li [a*]

a. Guangxi Key Laboratory of Clean Pulp & Papermaking and Pollution Control, College of Light Industry and Food Engineering, Guangxi University, Nanning 530004 (China).

b. Guangxi Key Laboratory of Natural Polymer Chemistry and Physics, College of Chemistry and Materials Science, Nanning Normal University, Nanning 530004 (China)

*Corresponding author

Wei Li (E-mail: weili@gxu.edu.cn)

Contents

1. Materials and methods

1.1 Materials

Unbleached eucalyptus pulp was obtained from Asia Symbol (Shangdong) Pulp and Paper Co., Ltd (Rizhao, China) with cellulose, hemicellulose and lignin content of 64.60%, 13.72%, and 13.16%, respectively. Sodium hydroxide (NaOH) was purchased from Shanghai Macklin Biochemical Co., Ltd (Shanghai, China). Sulfuric acid (H_2SO_4) was provided by Aladdin Biotechnology Co., Ltd (Shanghai, China). All the chemicals were used as received.

1.2 Preparation of lignocellulosic nanofibers

Unbleached eucalyptus pulp (200 g, dry weight) was soaked in deionized water for 12 h and then defibered by a disintegrator (AG 04, Estanit GmbH, Germany). The obtained slurry at a consistency of 2 wt% was further ground by using a superfine grinding mill (MKZA 10-15JIV, Masuko Sangyo, Japan). The grinding process was performed at a speed of 1500 rpm with a clearance of -100 μm and a total grinding time of 2 h. The resulting lignocellulosic nanofiber suspension was stored in a refrigerator at 4°C.

1.3 Preparation of lignocellulosic xerogel

The ligonocellulosic nanofiber suspension with a consistency of 2 wt% (the dry fiber weight of 1 g) was stirred for 30 min. NaOH solutions with concentrations of 12.5 wt%, 25 wt%, 50 wt% and 75 wt% (based on the dry weight of fibers) were separately added into the above suspension. After stirring at room temperature (RT) for 30 min, the mixtures were frozen at -20°C for 5 h and then thawed at RT, followed by washing with deionized water until the pH of the lignocellulosic hydrogels reached 7. Finally, the hydrogels were dried in an oven at 40°C for 24 h to obtain the corresponding xerogels, which were named as $X_{12.5}$, X_{25}, X_{50} and X_{75}, respectively. The xerogels prepared with

slurry concentrations of 2.5 wt% and 3.0 wt% with the same method at a NaOH content of 12.5 wt% were named as $C_{2.5}$ and C_3, respectively. Similarly, the xerogels prepared with different lignin contents were named as $X_{12.5\text{-}1}$, $X_{12.5\text{-}2}$, $X_{12.5\text{-}3}$ and $X_{12.5\text{-}4}$, respectively, and the fibers with different lignin contents were named as B_1, B_2, B_3 and B_4, respectively. Additionally, the xerogels prepared with different drying temperatures of 25°C, 60°C, 80°C, and 100°C were named as $X_{12.5\text{-}0\text{-}25}$, $X_{12.5\text{-}0\text{-}60}$, $X_{12.5\text{-}0\text{-}80}$, and $X_{12.5\text{-}0\text{-}100}$, respectively.

1.4 Characterization

The contents of cellulose, hemicellulose and lignin in fibers were determined by the National Renewable Energy Laboratory method (NREL method).[1] Raman spectra of the pristine fiber suspensions and the hydrogels were obtained using a laser Raman spectrometer (inVia Reflex, Renishaw, UK) with an excitation wavelength of 532 nm. The chemical structure of fibers and xerogels was analyzed by a Fourier transform infrared spectroscopy (ATR-FTIR; Bruker, Germany) with a scanning wavenumber range of 4000-500 cm^{-1} and X-ray photoelectron spectroscopy (XPS, ThermoFisher Scientific, the USA). The crystal structure of fibers and xerogels was measured by X-ray diffraction (XRD, SMARTLAB, Japan) with a scanning range of 2θ = 5-50°. Crystallinity (CrI) was calculated by equation (1):[2]

$$CrI(\%) = \frac{I_{002} - I_{am}}{I_{002}} \times 100 \quad (1)$$

where I_{002} is the diffraction intensity of the crystalline region at 2θ=22.1°, and I_{am} is the diffraction intensity of the amorphous region at 2θ=18.5°.

The volume shrinkage (%) of the xerogels after ambient drying was calculated using equation (2):

$$Volume\ shrinkage(\%) = \frac{V_0 - V}{V_0} \times 100 \quad (2)$$

Where V_0 is the initial volume of the hydrogel and V is the final volume of the xerogel after drying.

The density (ρ_a, g cm^{-3}) and porosity (Φ, %) of xerogels were calculated according to equation (3) and equation (4), respectively.[3]

$$\rho_a = \frac{m_a}{V_a} \quad (3)$$

$$\Phi = 100 \times (1 - \frac{\rho_a}{\rho_0}) \quad (4)$$

Where m_a (g) and V_a (cm^3) represent the mass and volume of the xerogel, respectively, and ρ_0 is the solid scaffold density of the xerogel (1.6754 g cm^{-3}).

The solid scaffold density and pore size of the xerogels were measured by a high-performance automatic mercury injection meter (Micromeritics AutoPore IV 9500, USA). Transmission electron microscopy (TEM, HT7700, Hitachi, Japan) and scanning electron microscopy (SEM, F16502, Phenom, Holland) were used to observe the morphology of the fibers and xerogels. The cross-section of the xerogels was stained using safranine O stain, and the distribution of lignin was observed using confocal laser scanning microscopy (CLSM, Leica TCS SP8). The mechanical properties of the xerogels were tested by a universal testing machine (3367U4830, Instron, UK) at a speed of 10 mm/min. The thermal conductivity of xerogels was determined by a thermal conductivity meter (TPS 2500S, Hot Disk, Sweden) using the transient plane heat source method. The infrared thermal images of xerogels were taken by an infrared thermal imager (FLIR E4, USA). The molecular dynamic (MD) simulation was carried out using GROMACS software (version 2021.1)[4] to investigate the hydrogen bond

changes of cellulose molecules in NaOH aqueous solution. The structures of the samples were optimized using the GROMOS56 force field.[5-8] A cellulose model consisting of 5 layers of cellulose chains, with 6 chains in each layer and a degree of polymerization (DP) of 8 for each chain. The cellulose chains, 122 sodium ions, 122

hydroxide ions, and 10575 water molecules were randomly dispersed in a box (9.49 nm × 9.49 nm × 4.152 nm). Energy minimization was carried out to optimize the structures by using the steepest descents followed by conjugate gradient methods. The equilibration and production run were both performed under the NPT ensemble (constant number of particles, pressure, and temperature) at 253.15 K and 1 bar. All bonds were constrained using the LINCS (Linear Constraint Solver) algorithm.[9] The short-range Coulomb and Lennard-Jones interactions were calculated under the cutoff distance of 1.4 nm,[10, 11] while the PME method was used for long-range Coulomb interactions.[12] The simulation employed v-rescale temperature coupling and the Berendsen pressure coupling method.[13, 14] The total production run lasted for 20 ns.

2. Table S1-S6

Table S1. The crystallinity (CrI) of pristine fibers and fibers treated by different NaOH freezing time as well as the lignocellulosic xerogels ($X_{12.5\text{-}75}$).

Samples	CrI (%)
pristine fibers	73.50
F-1	75.56
F-2	76.46
F-3	76.96
F-4	72.69
$X_{12.5}$	70.72
X_{25}	66.51
X_{50}	49.75
X_{75}	46.15

Table S2. Volume shrinkage ratio, density and porosity of lignocellulosic xerogels with different NaOH contents, slurry consistencies, lignin contents and drying temperature.

Samples	NaOH content (wt%)	Slurry consistency (%)	Drying temperature (°C)	Volume shrinkage ratio (%)	Density (mg cm^{-3})	Porosity (%)
$X_{12.5}$	12.5	2.0	40	27.50 ± 0.38	39.19 ± 1.05	97.57
X_{25}	25.0	2.0	40	32.28 ± 0.44	41.30 ± 0.91	97.28
X_{50}	50.0	2.0	40	39.98 ± 0.42	56.07 ± 0.86	96.65
X_{75}	75.0	2.0	40	47.33 ± 0.89	71.54 ± 1.15	95.73
$X_{12.5\text{-}1}$	12.5	2.0	40	31.65 ± 1.16	42.30 ± 0.19	97.48
$X_{12.5\text{-}2}$	12.5	2.0	40	33.83 ± 0.06	48.63 ± 0.65	97.10
$X_{12.5\text{-}3}$	12.5	2.0	40	35.25 ± 1.61	53.06 ± 0.82	96.83
$X_{12.5\text{-}4}$	12.5	2.0	40	36.71 ± 1.23	57.80 ± 0.28	96.55
$C_{2.5}$	12.5	2.5	40	26.40 ± 0.45	48.60 ± 1.12	97.10
C_3	12.5	3.0	40	24.68 ± 0.68	52.43 ± 1.00	96.87
$X_{12.5\text{-}0\text{-}25}$	12.5	2.0	25	31.57 ± 0.75	43.12 ± 0.92	97.43
$X_{12.5\text{-}0\text{-}60}$	12.5	2.0	60	32.88 ± 1.20	44.59 ± 0.32	97.34
$X_{12.5\text{-}0\text{-}80}$	12.5	2.0	80	36.34 ± 0.90	46.75 ± 0.10	97.21
$X_{12.5\text{-}0\text{-}100}$	12.5	2.0	100	36.98 ± 0.86	47.50 ± 0.08	97.16

Table S3. Chemical components of pristine fibers in different degrees of bleaching.

Samples	Cellulose (%)	Hemicellulose (%)	Lignin (%)
Pristine fibers	64.60	13.77	13.16
B1	62.23	12.83	9.27
B2	64.30	13.04	6.98
B3	65.51	12.33	5.37
B4	67.22	12.79	2.72

Table S4. Density and porosity of $X_{12.5}$ compared with reported cellulose-based xerogels.

Samples	Raw materials	Preparation methods	Density (g cm^{-3})	Porosity (%)	Reference
$Xero_{-0.72–2.5}$	MCC	DMF dissolution and MeOH regeneration	0.140	91.00	11
Cellulose xerogel	Cellulose	NaOH/urea dissolution and sulfuric acid regeneration	0.055	97.00	40
Xerogel	MCC	EMImAc/DMSO dissolution and MeOH regeneration	1.427	5.00	41
Nanocellulose xerogel	CNFs	Acid-induced gelation	-	71.00	12
CNF xerogel	CNFs	Vacuum filtration of CNF suspension	0.600	-	10
Cellulose xerogel	CNFs	Chemical crosslinking	0.059	-	16
$X_{12.5}$	Lignocellulosic fiber	NaOH freezing	0.039	97.57	This work

Table S5. Comparison of stress between reported cellulose aerogels and our designed lignocellulosic xerogel at 80% strain.

Materials	Stress (kPa)	Reference
CNF aerogel	142.5	44
LCNF aerogel	86.0	45
CMNC/bagasse aerogel	503.8	20
CNF/MTMS/FS aerogel	175.0	46
MXene/CNF aerogel	280.0	47
Nanocellulose aerogel	303.6	9
$X_{12.5}$	782.2	This work

Table S6. Density, porosity and drying time of xerogel and aerogel.

Samples	Density (mg cm^{-3})	Porosity (%)	Drying time (h)
$X_{12.5}$	39.19 ± 1.05	97.57	24
$A_{12.5}$	27.91 ± 0.26	98.34	48

2. Fig. S1-S10

Fig. S1 Pictures of pristine lignocellulose fibers and fibers treated by different NaOH freezing time.

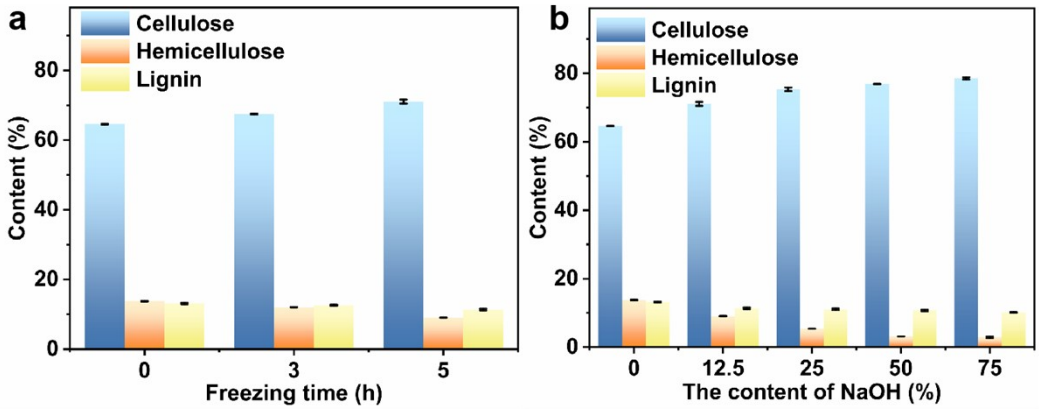

Fig. S2 a,b) Chemical components of pristine fibers and fibers treated by different NaOH freezing time (a) and $X_{12.5\text{-}75}$ (b).

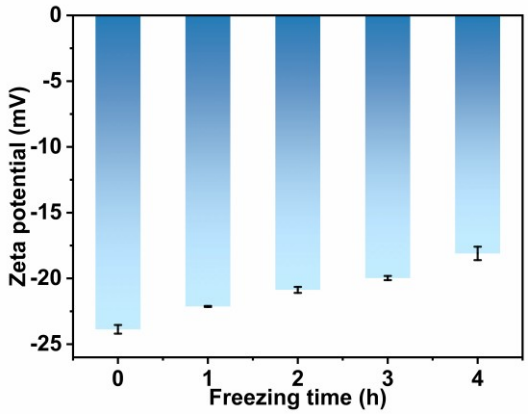

Fig. S3 Zeta potential of pristine fibers and fibers treated by different NaOH freezing time.

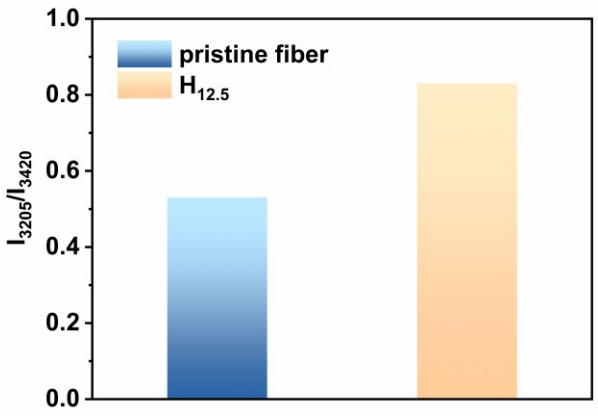

Fig. S4 Intensity ratio of 3205 cm^{-1} and 3420 cm^{-1} vibration bands (I_{3205}/I_{3435}) in the Raman spectra of the pristine fiber suspension and the lignocellulosic hydrogel ($H_{12.5}$).

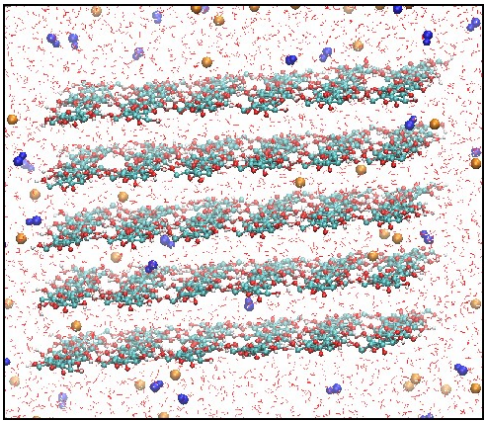

Fig. S5 The initial structure of cellulose molecules in NaOH aqueous solution

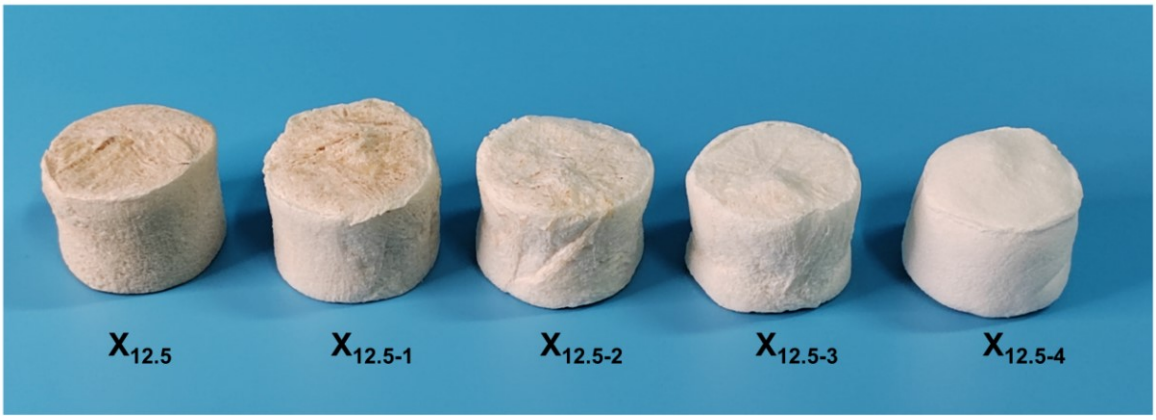

Fig. S6 Pictures of lignocellulosic xerogels with different lignin contents.

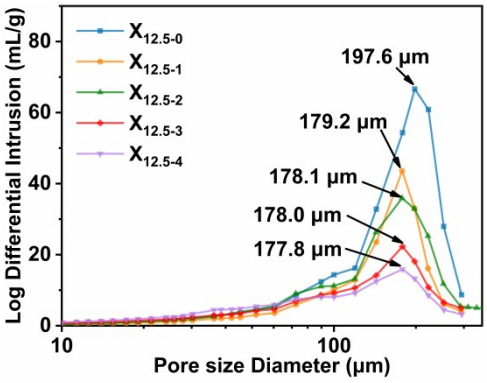

Fig. S7 Pore size of lignocellulosic xerogels with different lignin contents.

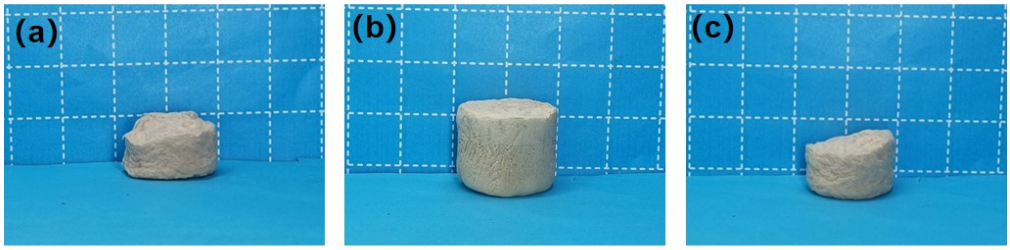

Fig. S8 Pictures of lignocellulosic xerogels prepared with different sizes of lignocellulosic fibers: pristine fibers (a), fibers after milling for 120 min (b), fibers after milling for 200 min (c).

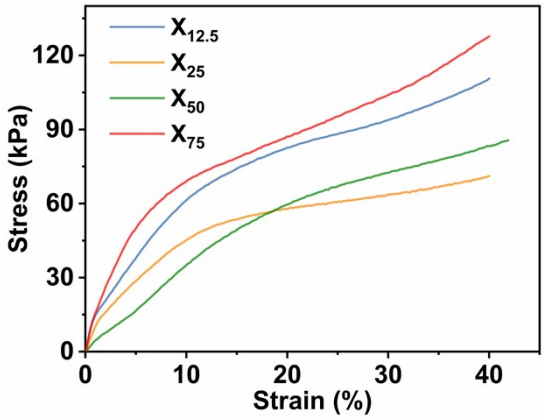

Fig. S9 Stress-strain curves of $X_{12.5\text{-}75}$ at 40% strain.

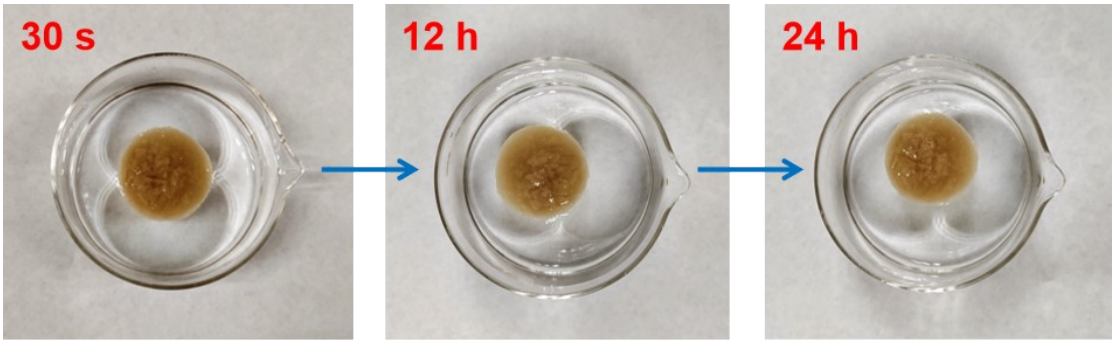

Fig. S10 Pictures of $X_{12.5}$ immersed in DI water for different time periods.

4. Reference

1. Y. D. Luo, Y. Li, L. M. Cao, J. T. Zhu, B. J. Deng, Y. J. Hou, C. Liang, C. X. Huang, C. R. Qin and S. Q. Yao, *Bioresour. Technol.*, 2021, **341**, 7.
2. P. Tao, Y. H. Zhang, Z. M. Wu, X. P. Liao and S. X. Nie, *Carbohydr. Polym.*, 2019, **214**, 1-7.
3. C. J. Xie, S. Y. Liu, Q. G. Zhang, H. X. Ma, S. X. Yang, Z. X. Guo, T. Qu and X. L. Tuo, *ACS Nano*, 2021, **15**, 10000-10009.
4. B. Hess, C. Kutzner, D. van der Spoel and E. Lindahl, *J. Chem. Theory Comput.*, 2008, **4**, 435-447.
5. P. Chen, Y. Nishiyama and K. Mazeau, *Cellulose*, 2014, **21**, 2207-2217.
6. H. S. Hansen and P. H. Hünenberger, *J. Comput. Chem.*, 2011, **32**, 998-1032.
7. J. S. Hub, M. G. Wolf, C. Caleman, P. J. Maaren, G. Groenhof and D. van der Spoel, *Chem. Sci.*, 2014, **5**, 1745-1749.
8. Y. Chen, X. T. Fu, S. X. Yu, K. Quan, C. J. Zhao, Z. Q. Shao, D. D. Ye, H. S. Qi and P. Chen, *J. Appl. Polym. Sci.*, 2021, **138**, 8.
9. B. Hess, H. Bekker, H. J. Berendsen and J. Fraaije, *Journal of J. Comput. Chem.*, 1997, **18**, 1463-1472.
10. T. Darden, D. York and L. Pedersen, *J. Chem. Phys.*, 1993, **98**, 10089-10092.
11. C. L. Wennberg, T. Murtola, B. Hess and E. Lindahl, *J. Chem. Theory Comput.*, 2013, **9**, 3527-3537.
12. M. J. Abraham and J. E. Gready, *J. Comput. Chem.*, 2011, **32**, 2031-2040.
13. G. Bussi, D. Donadio and M. Parrinello, *J. Chem. Phys.*, 2007, **126**, 7.
14. H. J. Berendsen, J. V. Postma and W. F. Van Gunsteren, *J. Chem. Phys.*, 1984, **81**, 3684-3690.